Scaling of the Nonlinear Coupling Coefficient in Multimode Fibers

Paolo Carniello[(1)], Filipe M. Ferreira[(2)], Norbert Hanik[(1)]

[(1)] Institute for Communications Engineering, Technische Universität München, paolo.carniello@tum.de
[(2)] Optical Networks, Dept. Electronic and Electrical Eng., University College London

Abstract *We derive approximate closed-form expressions and scaling rules for the fiber nonlinear coefficient $\gamma\kappa$ with the number of modes in strongly-coupled multimode fibers for space-division multiplexing.*

Introduction

In the field of space-division multiplexing (SDM) the most common fiber structures are multicore fibers (MCFs) and multimode fibers (MMFs). MCFs are considered to be the preferred medium for long-haul communications given their potential for smaller multiple-input multiple-output (MIMO) signal processing complexity, when compared to MMFs[1]–[3]. This is, in MCFs, the level of linear coupling can be directly controlled through, e.g., the separation of the cores[1],[3], to achieve weak coupling and avoid higher-order MIMO altogether, or to achieve strong coupling reducing the fiber delay spread[4] and so the MIMO receiver complexity[3]. However, MMFs allow for a higher spatial-spectral efficiency than that of MCFs[2], given their potential to support a larger number of spatial paths, even above 1000, in the same cross-sectional area of a single mode fiber (SMF). A strong motivation to the study of MMFs for long distances and, thus, bringing into play the Kerr nonlinear response of silica fibers.

In strongly-coupled SDM systems, Kerr nonlinearity is taken into account through the following Manakov equation[5],[6]:

$$\frac{\mathrm{d}\boldsymbol{A}}{\mathrm{d}z} = +\mathrm{L}\left[\boldsymbol{A}\right] - j\gamma\kappa\|\boldsymbol{A}\|^2\boldsymbol{A} \qquad (1)$$

where $\boldsymbol{A} = [A_1, \ldots, A_M]^T$ is the vector of modal amplitudes, and $\mathrm{L}\left[\boldsymbol{A}\right]$ is the linear operator accounting for mode coupling and dispersion. The last term of (1) accounts for Kerr effect, which depends on two coefficients $\gamma = \frac{\omega_0 n_2}{c\mathcal{A}_{11}}$ and $\kappa = \frac{4}{3}\frac{M}{M+1}\frac{\mathcal{A}_{11}}{(M/2)^2}\sum_{a=1}^{(M/2)}\sum_{b=1}^{(M/2)}\frac{1}{\mathcal{A}_{ab}}$, where M is the total number of modes (including polarizations), ω_0 is the central frequency, n_2 is the nonlinear refractive index, c is the light-speed in vacuum, $\mathcal{A}_{ab} = \frac{\iint|F_a|^2\,\mathrm{d}x\,\mathrm{d}y\iint|F_b^2|\,\mathrm{d}x\,\mathrm{d}y}{\iint|F_a|^2|F_b|^2\,\mathrm{d}x\,\mathrm{d}y}$ is the intermodal effective area between spatial modes $\boldsymbol{F_a}$ and $\boldsymbol{F_b}$[6].

For multimode SDM systems, the term $\gamma\kappa$ in (1) is sometimes assumed scaling as $1/M$, in which case, under certain scenarios, spectral efficiency per mode would increase with M[6]. However, as we show in the following, the assumption $\gamma\kappa \propto 1/M$ is valid only for a particular fiber design strategy, that is by increasing only the core radius.

Scaling of the Nonlinear Coefficient with Index Difference and Core Radius

Designing a MMF essentially consists in selecting the refractive index profile shape $n(r)$ (r is the radial coordinate), refractive index difference $\Delta = (n^2(0) - n^2(R))/(2n^2(0))$ (or numerical aperture $\mathrm{NA} = \sqrt{n^2(0) - n^2(R)}$), and core radius R, that allow for a given number of modes. We limit ourselves to the trenchless parabolic graded-index (GI) and step-index (SI) profiles[7]. To increase the number of modes ($M \gtrsim 200$), besides increasing R, one can increase Δ since it is a free parameter. In any case, a larger M comes with enhanced detrimental effects, such as modal delays, mode-dependent losses, and bend losses, for which tuning Δ can be helpful[2],[8]. Hence, we study the scaling of $\gamma\kappa$ in the general scenario where both R and Δ are varied, starting with the case in which only one of the two changes, keeping the other fixed. We choose Δ ranging from $\Delta_{\mathrm{min,GI}}$ or Δ_{GISMF}, for a graded-index single mode fiber (GISMF), to Δ_{max}; R from R_{GISMF} to R_{max}. A detailed explanation of the choice of these parameters is given later. We set $\lambda_0 = 1550\,\mathrm{nm}$, $k_0 = (2\pi)/\lambda_0$, $n_2 = 2.6\cdot 10^{-20}\,\mathrm{m^2W^{-1}}$, and assume weak-guidance.

Considering a set of graded-index multimode fibers (GIMMFs) for which R increases while Δ is held fixed, we derived an approximation for $\gamma\kappa$:

$$\gamma\kappa \approx \frac{\omega_0 n_2}{c}\frac{7}{4}\frac{(\mathrm{NA}k_0)^2}{4\pi M}. \qquad (2)$$

Fig.1 shows $\gamma\kappa$ as a function of M for analytical results (dashed lines) and for numerical results (markers) exploiting mode solver solutions[9] – M is varied by Δ and/or R . The accuracy of (2) (for $M > 2$) is self-evident from the matching between analytical and numerical results for the cases $\Delta = \Delta_{\mathrm{max}}$, and $\Delta = \Delta_{\mathrm{GISMF}}$. Eq.(2) was derived by independently approximating γ

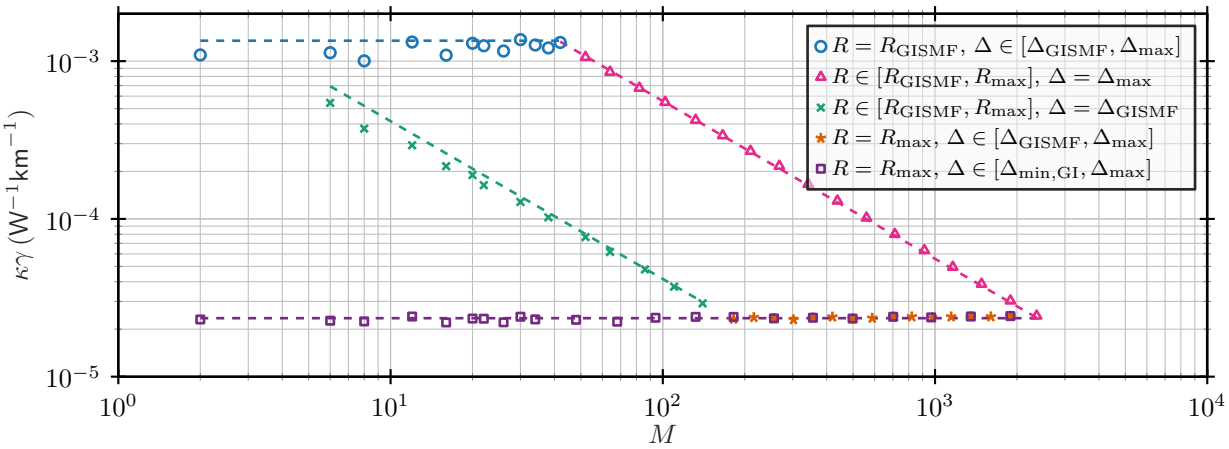

Fig. 1: Scaling of $\gamma\kappa$ with M for different GIMMF designs. The dashed lines are the proposed formulas: cyan is (3) with $R = R_{\mathrm{GISMF}}$; magenta is (2) with $\Delta = \Delta_{\max}$; green is (2) with $\Delta = \Delta_{\mathrm{GISMF}}$; violet is (3) with $R = R_{\max}$.

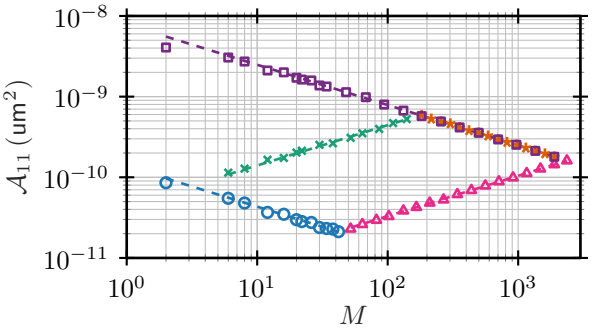

Fig. 2: Scaling of $\mathcal{A}_{11}$ with M for different GIMMF designs. The dashed lines are the proposed formulas. Same labels for lines and markers as in Fig.1.

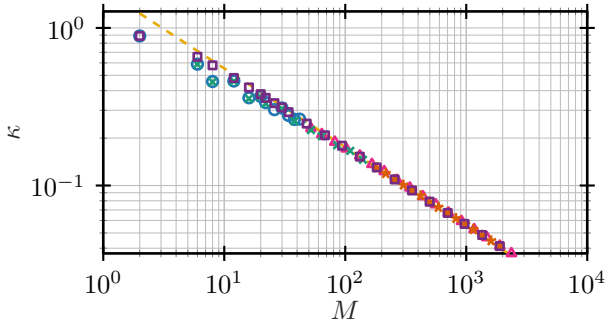

Fig. 3: Scaling of κ with M for different GIMMF designs. The yellow dashed line is the proposed fitted formula $7/(4\sqrt{M})$. Same marker labels as in Fig.1.

and κ. For γ, we exploited a Gaussian approximation for the fundamental mode[10],[11] to obtain $\mathcal{A}_{11} \approx \pi \frac{1}{(\mathrm{NA}k_0)^2} 4\sqrt{M}$, whose accuracy is visible in Fig.2. The intuition is that $\mathcal{A}_{11}$, which is a measure of how much a mode spreads over a fiber cross-section, increases with R. For κ, we fitted $\kappa \approx \frac{7}{4\sqrt{M}}$ from numerical simulations, see Fig.3. The intuition is that the inclusion of a larger number of modes with greater effective areas $\mathcal{A}_{kk}$ into the averaging procedure to compute κ, lowers κ.

For a set of GIMMFs with increasing Δ and fixed R, we derived:

$$\gamma\kappa \approx \frac{\omega_0 n_2}{c} \frac{7}{4} \frac{1}{\pi R^2} \qquad (3)$$

which indicates that $\gamma\kappa$ stays constant when Δ is varied. Fig.1 shows analytical and simulation results for $R = R_{\max}$ and $R = R_{\mathrm{GISMF}}$, confirming the validity of (3). Eq.(3) was derived by firstly exploiting again the Gaussian approximation to obtain $\mathcal{A}_{11} \approx \frac{\pi R^2}{\sqrt{M}}$. The intuition is that an increase of Δ tends to confine the modal profiles, hence $\mathcal{A}_{11}$ reduces. Secondly, the same fitted relation $\kappa \approx \frac{7}{4\sqrt{M}}$ as above was used. Both (2) and (3) are valid also when R and Δ are varied together. However, in such case the scaling of $\gamma\kappa$ with M is hidden behind NA and R, respectively.

For step-index multimode fibers (SIMMFs), it can be shown that the same trends hold, i.e., $\gamma\kappa \propto 1/M$ when Δ is fixed, and $\gamma\kappa \approx \mathrm{const}$ when R is fixed, although with less accuracy than for GIMMFs, see Fig.5.

Bounds on the Nonlinear Coefficient

The ultimate throughput limit depends on the overall impact of the Kerr nonlinearity. Towards the assessment of the potential throughput of SDM systems against a bundle of SMFs[1],[3], in the following we analyze the range of achievable values for $\gamma\kappa$ in MMFs. Starting from a baseline GISMF, the upper bound is obtained by increasing Δ from Δ_{GISMF} until $\Delta_{\max}$, and then increasing R from R_{GISMF} until $R_{\max}$. Finally, we study two lower bounds. One is found by increasing R from R_{GISMF} until $R_{\max}$, and then increasing Δ from Δ_{GISMF} until $\Delta_{\max}$. A more conservative lower bound, which accounts also for large mode area fibers, is found by assuming a reference fiber with $R = R_{\max}$ and $\Delta = \Delta_{\min,\mathrm{GI}}$, in which case Δ is increased up to $\Delta_{\max}$. We chose $R_{\mathrm{GISMF}} = 6.6\,\mu\mathrm{m}$ and $\Delta_{\mathrm{GISMF}} = 0.41\%$, so that $\mathcal{A}_{11} \approx 86\,\mu\mathrm{m}^2$, similar to a SSMF[12]. We set $\Delta_{\max} = 5\%$, $R_{\max} = 50\,\mu\mathrm{m}$, and $\Delta_{\min,\mathrm{GI}} = 0.0073\%$. Extreme Δ values are considered for maximum general-

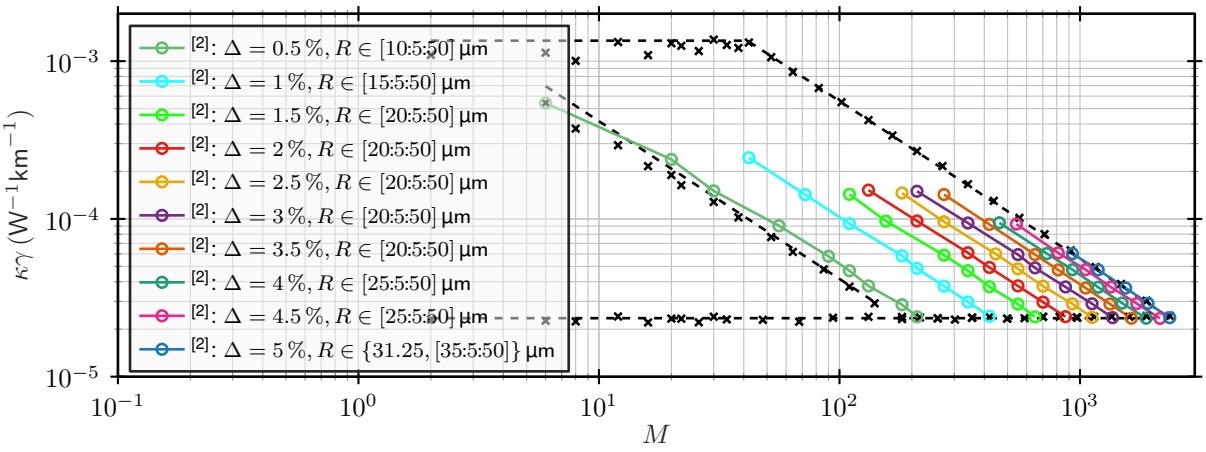

Fig. 4: Scaling of $\gamma\kappa$ with M for optimized fibers as in Ref.[2] (in colors). In black the same lines as Fig.1.

Tab. 1: Parameters for relevant GIMMFs in Fig.1

M	$\Delta\,(\%)$	$R\,(\mu\mathrm{m})$	$\mathcal{A}_{11}\,(\mu\mathrm{m}^2)$	κ	$\gamma\kappa\,(1/\mathrm{W/km})$
2	0.41	6.6	86	8/9	1.1
2	0.0073	50	4066	8/9	0.023
42	5.0	6.6	21	0.26	1.3
182	0.41	50	574	0.13	0.024
2562	5.0	50	161	0.037	0.024

ization. A higher $\Delta_{\max}$ would tend to break the weak-guidance approximation, and would not be practical since modal delays and mode-dependent losses would be too high[2]. The value of $R_{\max}$ was bound by fixing a $125\,\mu$m diameter cladding as for SMFs, for device backward compatibility[13], and mechanical reliability[2],[3],[13]. The bounds and the set of achievable values for $\gamma\kappa$ are visible in Fig.1. Table 1 summarizes parameters for relevant fibers in Fig.1.

The same procedure can be repeated for SIMMFs. As initial point it has been chosen a fiber with $R_{\mathrm{SISMF}} = 4.1\,\mu$m and $\Delta_{\mathrm{SISMF}} = 0.32\%$, to mimic a SSMF with $\mathcal{A}_{11} = 85\,\mu\mathrm{m}$[12]. The other relevant parameters are $R_{\max} = 50\,\mu$m, $\Delta_{\mathrm{min,SI}} = 0.0034\%$, and $\Delta_{\max} = 5\%$. The resulting bounds are visible in Fig.5.

The area of achievable values $\gamma\kappa$ in Fig.1 indicates that the scaling of $\gamma\kappa$ with M is not simply $1/M$, but depends on the strategy to increase M – subject to the consideration of the linear effects (e.g., modal dispersion)[2],[8]. The $\gamma\kappa \propto 1/M$ scaling can only be guaranteed for $M \lesssim 200$. Finally, a design strategy with poor $\gamma\kappa$ roll-off (with M), as for fixed R, may lead to enhanced nonlinearities.

Comparison with Optimized Fibers

In Fig.4 the $\gamma\kappa$ values for the GIMMFs designed as in Ref.[2] for low delay spread have been plotted against the results of the previous sections. The consistency between both sets of results supports the validity of our investigation. In particular, the optimized fibers lie within the foreseen boundaries,

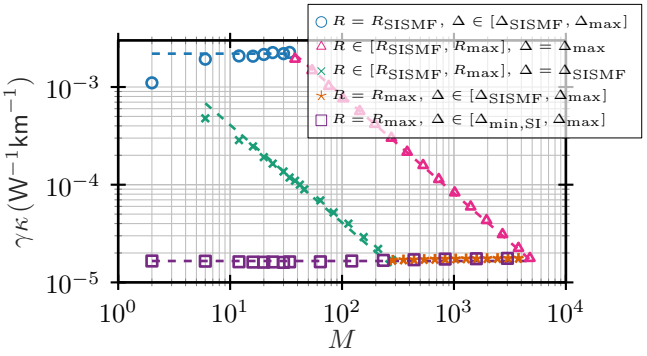

Fig. 5: Scaling of $\gamma\kappa$ with M for different SIMMF designs. The dashed lines are the discussed trends.

and the approximate trends for $\gamma\kappa$ ($\propto 1/M$ with R, and const with Δ), are verified again. Similar considerations hold for κ and $\mathcal{A}_{11}$. Finally, an analytic reasoning based on the Gaussian approximation indicates that for realistic slightly non-parabolic GIs, $\gamma\kappa$ deviates by at most 10% from the parabolic case.

Fiber data for this paper have been made freely available[14].

Conclusions

We studied the scaling of the nonlinear coefficient $\gamma\kappa$ with the number of modes in a MMF operating in the strongly coupled regime. Closed-form expressions for the scaling of $\gamma\kappa$ were proposed and validated against numerical results. These expressions can be used in throughput estimation models for SDM, e.g., GN-like models[15]. Thus, contributing towards the assessment of the feasibility of future long-haul SDM communication systems.

Acknowledgements

We acknowledge financial support by the Federal Ministry of Education and Research of Germany in the programme of “Souverän. Digital. Vernetzt.”. Joint project 6G-life, project identification number: 16KISK002. And, a UKRI Future Leaders Fellowship [grant number MR/T041218/1].

References

[1] G. M. Saridis, D. Alexandropoulos, G. Zervas, and D. Simeonidou, "Survey and evaluation of space division multiplexing: From technologies to optical networks", *IEEE Communications Surveys & Tutorials*, vol. 17, no. 4, pp. 2136–2156, 2015. DOI: 10.1109/COMST.2015.2466458.

[2] F. M. Ferreira and F. A. Barbosa, *Towards 1000-mode optical fibres*, 2022. arXiv: 2206.09855 [physics.optics].

[3] B. J. Puttnam, G. Rademacher, and R. S. Luís, "Space-division multiplexing for optical fiber communications", *Optica*, vol. 8, no. 9, pp. 1186–1203, Sep. 2021. DOI: 10.1364/OPTICA.427631.

[4] J. M. Kahn, K.-P. Ho, and M. B. Shemirani, "Mode coupling effects in multi-mode fibers", in *OFC/NFOEC*, 2012, pp. 1–3. DOI: https://doi.org/10.1364/ofc.2012.ow3d.3.

[5] S. Mumtaz, R.-J. Essiambre, and G. P. Agrawal, "Nonlinear propagation in multimode and multicore fibers: Generalization of the manakov equations", *Journal of Lightwave Technology*, vol. 31, no. 3, pp. 398–406, 2013. DOI: 10.1109/JLT.2012.2231401.

[6] C. Antonelli, M. Shtaif, and A. Mecozzi, "Modeling of nonlinear propagation in space-division multiplexed fiber-optic transmission", *Journal of Lightwave Technology*, vol. 34, no. 1, pp. 36–54, 2016. DOI: 10.1109/JLT.2015.2510511.

[7] G. Keiser, *Optical Fiber Communications, Fourth Edition*. McGraw-Hill, 2011.

[8] P. Sillard, M. Bigot-Astruc, and D. Molin, "Few-mode fibers for mode-division-multiplexed systems", *Journal of Lightwave Technology*, 2014. DOI: https://doi.org/10.1109/jlt.2014.2312845.

[9] T. Kernetsky, "Numerical optimization of ultra-broadband wavelength conversion in nonlinear optical waveguides", To be published, Ph.D. dissertation, Technische Universität München, 2022.

[10] D. Marcuse, "Loss analysis of single-mode fiber splices", *The Bell System Technical Journal*, vol. 56, no. 5, pp. 703–718, 1977. DOI: 10.1002/j.1538-7305.1977.tb00534.x.

[11] D. Marcuse, "Gaussian approximation of the fundamental modes of graded-index fibers", *The Journal of the Optical Society of America*, vol. 68, no. 1, pp. 103–109, Jan. 1978. DOI: 10.1364/JOSA.68.000103.

[12] *Corning smf-28e+ optical fiber*, Product Information, Corning Incorporated, Nov. 2021. [Online]. Available: https://www.corning.com/media/worldwide/coc/documents/Fiber/product-information-sheets/PI1463_07-14_English.pdf.

[13] R. Ryf and C. Antonelli, "Space-division multiplexing", *Springer Handbook of Optical Networks*, pp. 353–393, 2020. DOI: https://doi.org/10.1007/978-3-030-16250-4_10.

[14] P. Carniello and F. M. Ferreira, *Nonlinearity coefficients of multimode fibers*, Dataset, 2023. DOI: https://doi.org/10.14459/2023mp1707355. [Online]. Available: https://mediatum.ub.tum.de/1707355.

[15] P. Serena, C. Lasagni, A. Bononi, C. Antonelli, and A. Mecozzi, "The ergodic gn model for space-division multiplexing with strong mode coupling", *Journal of Lightwave Technology*, 2022. DOI: https://doi.org/10.1109/jlt.2022.3160207.